microbial function spanning terrestrial ecosystems, and though plant inputs are the dominant source of organic matter, vertebrate corpse inputs can be important resources (*5*, *6*). For example, one rain forest in Panama was estimated to receive 750 kg in mammal corpses annually per square kilometer (*12*). Although this represents less than 1% of the mass of plant litter received by another Panamanian rain forest (*13*), corpse nutrient sources can be an order of magnitude more concentrated than plant litter (*5*), and direct comparisons between plant and animal decomposition resources are rare (*14*). Thus, much is still unclear about the role of corpse inputs in larger-scale biogeochemical cycling (e.g., global carbon and nitrogen cycling) and in supporting specific communities and microbial diversity (*14*), and our results provide an important microbial perspective.

A societal impact of these results is the value of microbial data as physical evidence in medico-legal death investigation. We show that decomposer microbial communities could potentially serve as temporal (succession-based) and spatial (origin-based) (supplementary text) forms of physical evidence, such as the time elapsed since death (PMI) and the location of death. Our observation that postmortem microbial communities changed in a clock-like manner that provided an estimate of absolute PMI is similar to using the development of fly larvae to estimate PMI. However, the fly larvae PMI proxy is limited by corpse accessibility and season, resulting in PMI estimates in the range of weeks, months, and even years (*15*). Taken together, our findings demonstrate that postmortem microorganisms can provide both spatial and temporal insight into the events surrounding death.

REFERENCES AND NOTES

1. J. A. Gilbert, J. D. Neufeld, *PLOS Biol.* **12**, e1002020 (2014).
2. R. R. Parmenter, J. A. MacMahon, *Ecol. Monogr.* **79**, 637–661 (2009).
3. M. Swift, O. Heal, J. Anderson, *Decomposition in Terrestrial Ecosystems* (Blackwell Scientific, Oxford, 1979).
4. J. C. Moore et al., *Ecol. Lett.* **7**, 584–600 (2004).
5. D. O. Carter, D. Yellowlees, M. Tibbett, *Naturwissenschaften* **94**, 12–24 (2007).
6. P. S. Barton, in *Carrion Ecology, Evolution, and Their Applications*, M. E. Benbow, J. K. Tomberlin, A. M. Tarone, Eds. (CRC Press, 2015), pp. 273–292.
7. J. L. Metcalf et al., *eLife* **2**, e01104 (2013).
8. J. L. Pechal et al., *Int. J. Legal Med.* **128**, 193–205 (2014).
9. E. R. Hyde, D. P. Haarmann, J. F. Petrosino, A. M. Lynne, S. R. Bucheli, *Int. J. Legal Med.* **129**, 661–671 (2015).
10. W. E. D. Evans, *The Chemistry of Death* (Charles C Thomas, Springfield, IL, 1963).
11. M. G. I. Langille et al., *Nat. Biotechnol.* **31**, 814–821 (2013).
12. D. Houston, in *Neotropical Ornithology* (American Ornithologists' Union Monograph no. 36, Washington, DC, 1985), pp. 856–864.
13. M. Kaspari et al., *Ecol. Lett.* **11**, 35–43 (2008).
14. P. S. Barton, S. A. Cunningham, D. B. Lindenmayer, A. D. Manning, *Oecologia* **171**, 761–772 (2013).
15. J. Amendt et al., *Int. J. Legal Med.* **121**, 90–104 (2007).

ANCIENT MICROBIOME

The 5300-year-old *Helicobacter pylori* genome of the Iceman

Frank Maixner,[1]*† Ben Krause-Kyora,[2]† Dmitrij Turaev,[3]† Alexander Herbig,[4,5]† Michael R. Hoopmann,[6] Janice L. Hallows,[6] Ulrike Kusebauch,[6] Eduard Egarter Vigl,[7] Peter Malfertheiner,[8] Francis Megraud,[9] Niall O'Sullivan,[1] Giovanna Cipollini,[1] Valentina Coia,[1] Marco Samadelli,[1] Lars Engstrand,[10] Bodo Linz,[11] Robert L. Moritz,[6] Rudolf Grimm,[12] Johannes Krause,[4,5]‡ Almut Nebel,[2]‡ Yoshan Moodley,[13,14]‡ Thomas Rattei,[3]‡ Albert Zink[1]*‡

The stomach bacterium *Helicobacter pylori* is one of the most prevalent human pathogens. It has dispersed globally with its human host, resulting in a distinct phylogeographic pattern that can be used to reconstruct both recent and ancient human migrations. The extant European population of *H. pylori* is known to be a hybrid between Asian and African bacteria, but there exist different hypotheses about when and where the hybridization took place, reflecting the complex demographic history of Europeans. Here, we present a 5300-year-old *H. pylori* genome from a European Copper Age glacier mummy. The "Iceman" *H. pylori* is a nearly pure representative of the bacterial population of Asian origin that existed in Europe before hybridization, suggesting that the African population arrived in Europe within the past few thousand years.

The highly recombinant pathogen *Helicobacter pylori* has evolved to live in the acidic environment of the human stomach (*1*). Today, this Gram-negative bacterium is found in approximately half the world's human population, but fewer than 10% of carriers develop disease that manifests as stomach ulcers or gastric carcinoma (*2*, *3*). Predominant intrafamilial transmission of *H. pylori* and the long-term association with humans has resulted in a phylogeographic distribution pattern of *H. pylori* that is shared with its host (*4*, *5*). This observation suggests that the pathogen not only accompanied modern humans out of Africa (*6*), but that it has also been associated with its host for at least 100,000 years (*7*). Thus, the bacterium has been used as a marker for tracing complex demographic events in human prehistory (*4*, *8*, *9*). Modern *H. pylori* strains have been assigned to distinct populations according to their geographic origin (hpEurope, hpSahul, hpEastAsia, hpAsia2, hpNEAfrica, hpAfrica1, and hpAfrica2) that are derived from at least six ancestral sources (*4*, *5*, *8*).

The modern *H. pylori* strain found in most Europeans (hpEurope) putatively originated from recombination of the two ancestral populations Ancestral Europe 1 and 2 (AE1 and AE2) (*6*). It has been suggested that AE1 originated in Central Asia, where it evolved into hpAsia2, which is commonly found in South Asia. On the other hand, AE2 appears to have evolved in northeast Africa and hybridized with AE1 to become hpEurope (*4*). However, the precise hybridization zone of the parental populations and the true origin of hpEurope are controversial. Early studies observed a south-to-north cline in AE2/AE1 frequency in Europe (*4*, *6*). This finding has been attributed to independent peopling events that introduced these ancestral *H. pylori* components, which eventually recombined in Europe since the Neolithic period. More recently, it has been suggested that the AE1/AE2 admixture might have occurred in the Middle East or Western Asia between 10,000 and 52,000 years ago and that recombinant strains were introduced into Europe with the first human recolonizers after the last glacial maximum (*7*).

In this study, we screened 12 biopsy samples from the gastrointestinal tract of the Iceman, a 5300-year-old Copper Age mummy, for the presence of *H. pylori*. Stable isotope analyses showed that the Iceman originated and lived in Southern Europe, in the Eastern Italian Alps (*10*). Genetically, he most closely resembles early European farmers (*11–13*). The Iceman's stomach was discovered in a reappraisal of radiological data and contains the food he ingested shortly before his death (Fig. 1) (*14*). The study material included stomach content, mucosa tissue, and content of the small and large intestines (table S1). By using direct polymerase chain reaction (PCR), metagenomic diagnostics, and targeted genome capture (figs. S1 and S2), we determined the presence of *H. pylori* and reconstructed its complete genome.

Metagenomic analysis yielded endogenous ancient *H. pylori* DNA (15,350 reads) in all gastrointestinal tract contents (Fig. 1 and table S4). A control data set derived from Iceman's muscle tissue was negative. The distribution of the observed read counts throughout the Iceman's intestinal tract is similar to that in modern *H. pylori*–positive humans, with abundance decreasing from the stomach toward the lower intestinal tract (*15, 16*). The retrieved unambiguous reads were aligned to a modern *H. pylori* reference genome (strain 26695) and showed damage patterns indicative of ancient DNA (fig. S7) (*17*). After DNA repair, the *H. pylori* DNA was enriched up to 216-fold by using in-solution hybridization capture (Agilent) (fig. S5). From this data set, 499,245 nonredundant reads mapped to 92.2% of the 1.6-Mb *H. pylori* reference

genome with an 18.9-fold average coverage (Fig. 2). In comparison with the reference, the Iceman's ancient *H. pylori* genome had ~43,000 single-nucleotide polymorphisms (SNPs) and 39 deletions that range from 95 base pair (bp) to 17 kb and mainly comprise complete coding regions. Owing to deletions, the number of genomic variants is slightly below the range of what can be observed between modern *H. pylori* strains (table S13). The analysis of SNP allele frequencies does not indicate an infection by more than one strain (supplementary materials S6). In addition, as expected for this highly recombinant bacterium, we found evidence for gene insertions from *H. pylori* strains that differ from the reference genome (details about the InDels are provided in supplementary materials S8).

[1]Institute for Mummies and the Iceman, European Academy of Bozen/Bolzano (EURAC), Viale Druso 1, 39100 Bolzano, Italy. [2]Institute of Clinical Molecular Biology, Kiel University, Schittenhelmstrasse 12, 24105 Kiel, Germany. [3]CUBE–Division of Computational Systems Biology, Department of Microbiology and Ecosystem Science, University of Vienna, Althanstrasse 14, 1090 Vienna, Austria. [4]Institute for Archaeological Sciences, University of Tübingen, Rümelinstrasse 23, 72072 Tübingen, Germany. [5]Max Planck Institute for the Science of Human History, Kahlaische Strasse 10, 07745 Jena, Germany. [6]Institute for Systems Biology, 401 Terry Avenue North, Seattle, WA 98109, USA. [7]Scuola Superiore Sanitaria Provinciale "Claudiana," Via Lorenz Böhler 13, 39100 Bolzano, Italy. [8]Department of Gastroenterology, Hepatology, and Infectious Diseases, Otto-von-Guericke University, Leipziger Strasse 44, 39120 Magdeburg, Germany. [9]Université de Bordeaux, Centre National de Référence des Helicobacters et Campylobacters and INSERM U853, 146 rue Léo Saignat, 33076 Bordeaux, France. [10]Department of Microbiology, Tumor and Cell Biology, Karolinska Institutet, 141 83 Stockholm, Sweden. [11]Department of Veterinary and Biomedical Sciences, Pennsylvania State University, University Park, PA 16802, USA. [12]Robert Mondavi Institute for Food Science, University of California, Davis, CA 95616, USA. [13]Department of Zoology, University of Venda, Private Bag X5050, Thohoyandou 0950, Republic of South Africa. [14]Department of Integrative Biology and Evolution, Konrad Lorenz Institute for Ethology, University of Veterinary Medicine Vienna, Savoyenstrasse 1a, 1160 Vienna, Austria.
*Corresponding author. E-mail: frank.maixner@eurac.edu (F.M.); albert.zink@eurac.edu (A.Z.) †These authors contributed equally to this work. ‡These authors contributed equally to this work.
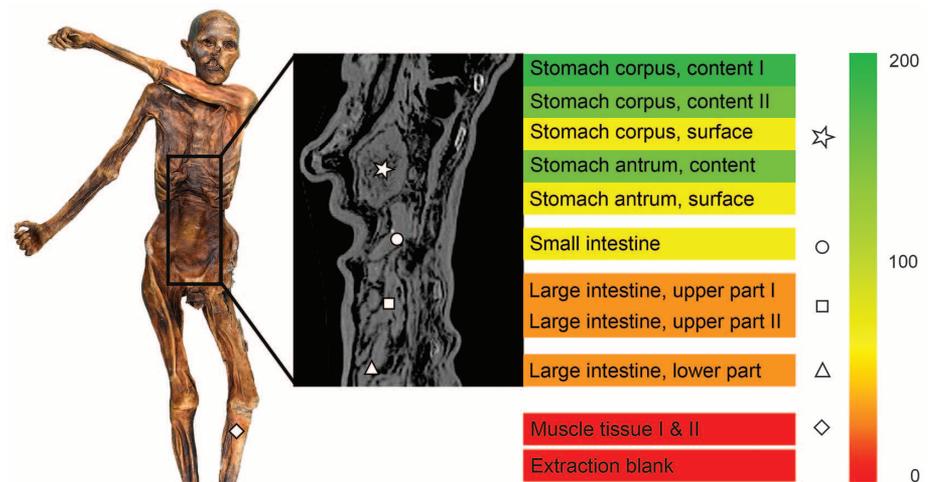
Fig. 1. *H. pylori*–specific reads detected in the metagenomic data sets of the Iceman's intestine content samples. The color gradient displays the number of unambiguous *H. pylori* reads per million metagenomic reads. Control metagenomic data sets of the Iceman's muscle tissue and of the extraction blank were included in the analysis. The different intestinal content sampling sites are marked in the radiographic image by the following symbols: asterisk, stomach content; circle, small intestine; square, upper large intestine; triangle, lower large intestine. The sampling site of the muscle control sample is highlighted in the Iceman overview picture (diamond).

Fig. 2. Gene coverage and distribution of the enriched and validated Iceman *H. pylori* reads mapped onto the 1.6 Mb large reference genome *H. pylori* 26695. The coverage plot displayed in black is superimposed onto the genomic plot. The bar on the right-hand side indicates a coverage of up to 50×. The gene coding sequences are shown in blue (positive strand) and yellow (negative strand) bars in the genomic plot. The loci of the ribosomal RNA genes, of two virulence genes (*vacA* and *cagA*), and of seven genes used for MLST analysis are highlighted in the genome plot.
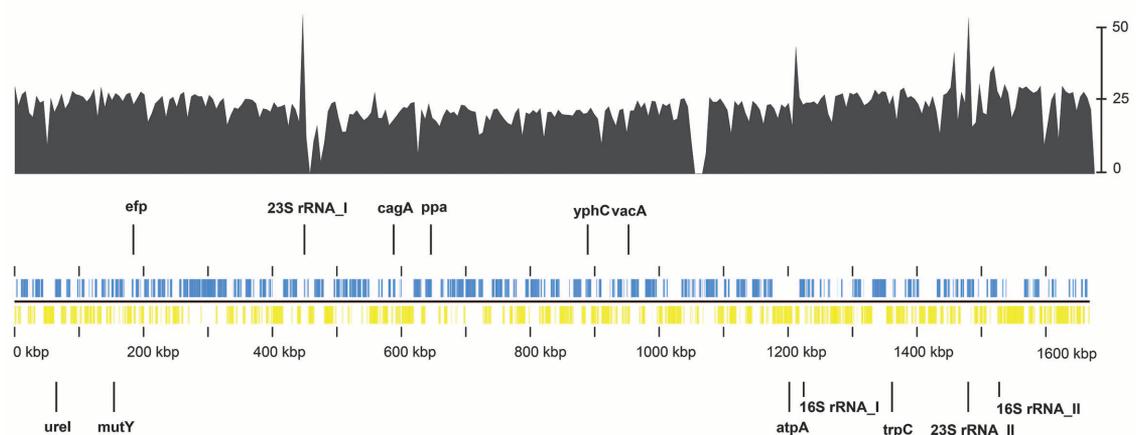
Fig. 3. Multilocus sequence analyses. (A) Bayesian cluster analysis performed in STRUCTURE displays the population partitioning of hpEurope, hpAsia2, and hpNEAfrica and the Iceman's *H. pylori* strain (details about the worldwide population partitioning of 1603 reference *H. pylori* strains are available in fig. S14). **(B)** STRUCTURE linkage model analysis showing the proportion of Ancestral Europe 1 (from Central Asia) and Ancestral Europe 2 (from northeast Africa) nucleotides among strains assigned to populations hpNEAfrica, hpEurope, and hpAsia2 and the Iceman's *H. pylori* strain on the extreme right. The black arrows indicate the position of the three extant European hpAsia2 strains. **(C)** Principal component analysis of contemporary hpNEAfrica, hpEurope, and hpAsia2 strains and the Iceman's *H. pylori* strain.
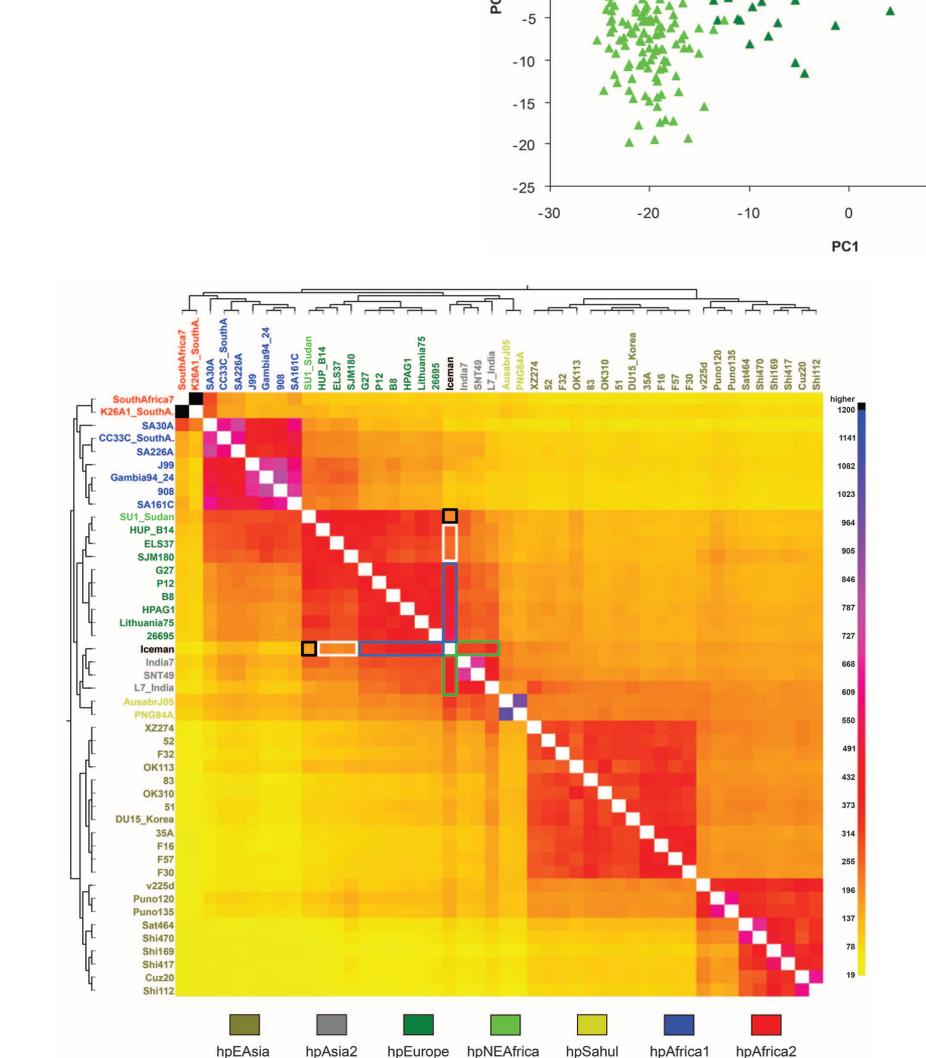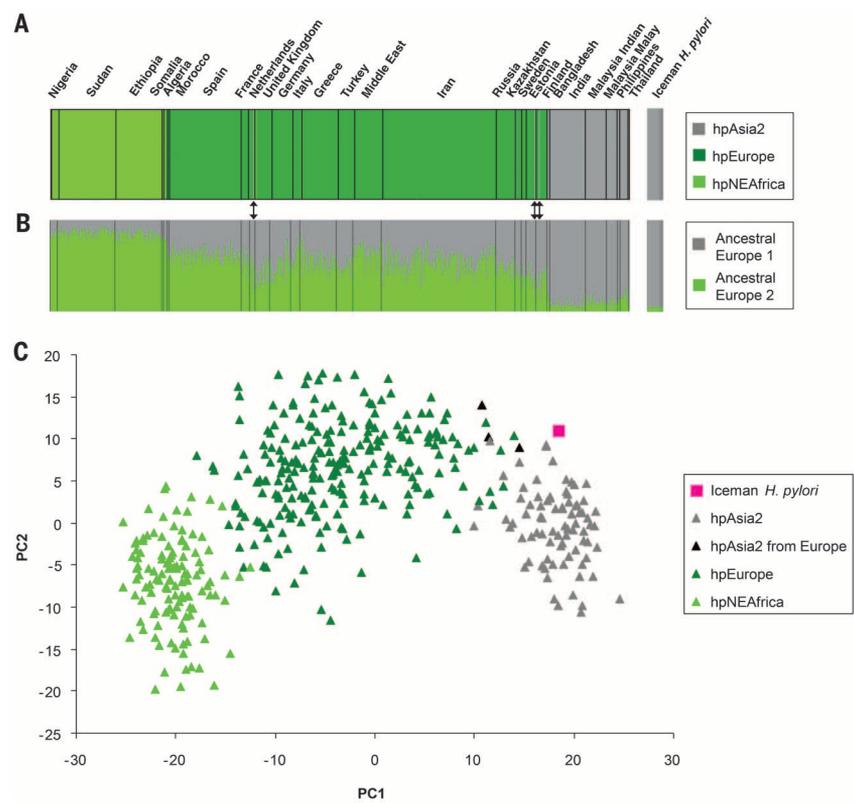

Fig. 4. Comparative whole-genome analysis. Co-ancestry matrix showing *H. pylori* population structure and genetic flux. The color in the heat map corresponds to the number of genomic motifs imported from a donor genome (column) to a recipient genome (row). The inferred tree and the *H. pylori* strain names are displayed on the top and left of the heat map. Strain names are colored according to the *H. pylori* population assignment provided in the legend below the heat map. Signs for population ancestry are highlighted in the heat map with green, blue, black, and white boxes.

Subsequent sequence analysis classified the ancient *H. pylori* as a *cagA*-positive *vacA* s1a/i1/m1 type strain that is now associated with inflammation of the gastric mucosa (fig. S11) (*18*). Using multistep solubilization and fractionation proteomics, we identified 115 human proteins in the stomach metaproteome, of which six were either highly expressed in the stomach mucosa (trefoil factor 2) (*19*) or present in the gastrointestinal tract and involved in digestion (supplementary materials S10). The majority of human proteins were enriched in extracellular matrix organizing proteins ($P = 3.35 \times 10^{-14}$) and proteins of immune processes ($P = 2 \times 10^{-3}$) (fig. S13). In total, 22 proteins observed in the Iceman stomach proteome are primarily expressed in neutrophils and are involved in the inflammatory host response. The two subunits S100A8 and S100A9 of calprotectin (CP) were detected with the highest number of distinct peptide hits in both analyzed samples. Inflamed gastric tissues of modern *H. pylori*–infected patients also show high levels of CP subunit S100A8 and S100A9 expression (*20*, *21*). Thus, the Iceman's stomach was colonized by a cytotoxic *H. pylori*–type strain that triggered CP release as a result of host inflammatory immune responses. However, whether the Iceman suffered from gastric disease cannot be determined from our analysis owing to the poor preservation of the stomach mucosa (fig. S3).

Comparative analysis of seven housekeeping gene fragments with a global multilocus sequence typing (MLST) database of 1603 *H. pylori* strains with the STRUCTURE (*22*) no-admixture model assigned the 5300-year-old bacterium to the modern population hpAsia2, commonly found in Central

and South Asia (Fig. 3A and fig. S14). The detection of an hpAsia2 strain in the Iceman's stomach is rather surprising because despite intensive sampling, only three hpAsia2 strains have ever been detected in modern Europeans. Stomachs of modern Europeans are predominantly colonized by recombinant hpEurope strains. Further analysis with the STRUCTURE linkage model (*23*), used to detect ancestral structure from admixture linkage disequilibrium, revealed that the ancient *H. pylori* strain contained only 6.5% [95% probability intervals (PI) 1.5 to 13.5%] of the northeast African (AE2) ancestral component of hpEurope (Fig. 3B). Among European strains, this low proportion of AE2 is distinct and has thus far only been observed in hpAsia2 strains from India and Southeast Asia. In contrast, the three European hpAsia2 strains (Fig. 3B, black arrows) contained considerably higher AE2 ancestries than that of the *H. pylori* strain of the Iceman (Finland 13.0%, PI 5.9 to 21.7; Estonia 13.2%, PI 6.2 to 22.3; and the Netherlands 20.8%, PI 11.5 to 31.7), although 95% probability intervals did overlap. A principal component analysis (PCA) of the MLST sequences of the hpAsia2, hpEurope, and hpNEAfrica populations revealed a continuum along PC1 that correlates with the proportion of AE2 ancestry versus AE1 ancestry of the isolates (Fig. 3C). The Iceman's ancient *H. pylori* was separated from modern hpEurope strains, and its position along PC1 was close to modern hpAsia2 strains from India, reflecting its almost pure AE1 and very low AE2 ancestry.

Comparative whole-genome analyses (neighbor joining, STRUCTURE, and principle component analyses) with publicly available genomes (*n* = 45) confirmed the MLST result by showing that the Iceman's ancient *H. pylori* genome has highest similarity to three hpAsia2 genomes from India (figs. S15 to S17). Although the Iceman's *H. pylori* strain appears genetically similar to the extant strains from northern India, slight differences were observed along PC2 in both MLST (Fig. 3C) and genome PCAs (fig. S17) and in the neighbor joining tree (fig. S15). To further study genomic-scale introgression, we performed a high-resolution analysis of ancestral motifs using fineSTRUCTURE (*24*). The resulting linked co-ancestry matrix (Fig. 4) showed that the ancient *H. pylori* genome shares high levels of ancestry with Indian hpAsia2 strains (Fig. 4, green boxes), but even higher co-ancestry with most European hpEurope strains (Fig. 4, blue boxes). In contrast, the Iceman's *H. pylori* shares low ancestry with the hpNEAfrica strain, a modern representative of AE2 (Fig. 4, black box), and with European strains originating from the Iberian Peninsula, where the proportion of AE2 ancestry is relatively high (Fig. 4, white box) (*4*). Our sample size (*n* = 1) does not allow further conclusions about the prevalence of AE1 in ancient Europe and the course or rate of AE2 introgression. However, the ancient *H. pylori* strain provides the first evidence that AE2 was already present in Central Europe during the Copper Age, albeit at a low level. If the Iceman *H. pylori* strain is representative of its time, the low level of AE2 admixture suggests that most of the AE2 ancestry observed in hpEurope today is a result of AE2 introgression into

Europe after the Copper Age, which is later than previously proposed (*4*, *6*). Furthermore, our co-ancestry results indicate that the Iceman's strain belonged to a prehistoric European branch of hpAsia2 that is different from the modern hpAsia2 population from northern India. The high genetic similarity of the ancient strain to bacteria from Europe implies that much of the diversity present in Copper Age Europe is still retained within the extant hpEurope population, despite millennia of subsequent AE2 introgression.

REFERENCES AND NOTES

1. S. Suerbaum, C. Josenhans, *Nat. Rev. Microbiol.* **5**, 441–452 (2007).
2. P. Malfertheiner, F. K. Chan, K. E. McColl, *Lancet* **374**, 1449–1461 (2009).
3. R. M. Peek Jr., M. J. Blaser, *Nat. Rev. Cancer* **2**, 28–37 (2002).
4. D. Falush *et al.*, *Science* **299**, 1582–1585 (2003).
5. Y. Moodley, B. Linz, *Genome Dyn.* **6**, 62–74 (2009).
6. B. Linz *et al.*, *Nature* **445**, 915–918 (2007).
7. Y. Moodley *et al.*, *PLOS Pathog.* **8**, e1002693 (2012).
8. Y. Moodley *et al.*, *Science* **323**, 527–530 (2009).
9. T. Wirth *et al.*, *Proc. Natl. Acad. Sci. U.S.A.* **101**, 4746–4751 (2004).
10. W. Müller, H. Fricke, A. N. Halliday, M. T. McCulloch, J. A. Wartho, *Science* **302**, 862–866 (2003).
11. W. Haak *et al.*, *Nature* **522**, 207–211 (2015).
12. A. Keller *et al.*, *Nat. Commun.* **3**, 698 (2012).
13. I. Lazaridis *et al.*, *Nature* **513**, 409–413 (2014).
14. P. Gostner, P. Pernter, G. Bonatti, A. Graefen, A. R. Zink, *Arch. Sci.* **38**, 3425–3431 (2011).
15. A. F. Andersson *et al.*, *PLOS ONE* **3**, e2836 (2008).
16. N. Segata *et al.*, *Genome Biol.* **13**, R42 (2012).
17. S. Sawyer, J. Krause, K. Guschanski, V. Savolainen, S. Pääbo, *PLOS ONE* **7**, e34131 (2012).
18. K. R. Jones, J. M. Whitmire, D. S. Merrell, *Front. Microbiol.* **1**, 115 (2010).
19. M. Uhlén *et al.*, *Science* **347**, 1260419 (2015).
20. J. A. Gaddy *et al.*, *PLOS Pathog.* **10**, e1004450 (2014).
21. S. T. Leach, H. M. Mitchell, C. L. Geczy, P. M. Sherman, A. S. Day, *Can. J. Gastroenterol.* **22**, 461–464 (2008).
22. J. K. Pritchard, M. Stephens, P. Donnelly, *Genetics* **155**, 945–959 (2000).
23. D. Falush, M. Stephens, J. K. Pritchard, *Genetics* **164**, 1567–1587 (2003).
24. D. J. Lawson, G. Hellenthal, S. Myers, D. Falush, *PLOS Genet.* **8**, e1002453 (2012).

PALEOCLIMATE

Reconciliation of the Devils Hole climate record with orbital forcing

Gina E. Moseley,[1]* R. Lawrence Edwards,[2] Kathleen A. Wendt,[1,2] Hai Cheng,[2,3] Yuri Dublyansky,[1] Yanbin Lu,[2] Ronny Boch,[1]† Christoph Spötl[1]

The driving force behind Quaternary glacial-interglacial cycles and much associated climate change is widely considered to be orbital forcing. However, previous versions of the iconic Devils Hole (Nevada) subaqueous calcite record exhibit shifts to interglacial values ~10,000 years before orbitally forced ice age terminations, and interglacial durations ~10,000 years longer than other estimates. Our measurements from Devils Hole 2 replicate virtually all aspects of the past 204,000 years of earlier records, except for the timing during terminations, and they lower the age of the record near Termination II by ~8000 years, removing both ~10,000-year anomalies. The shift to interglacial values now broadly coincides with the rise in boreal summer insolation, the marine termination, and the rise in atmospheric CO_2, which is consistent with mechanisms ultimately tied to orbital forcing.

Changes to Earth's orbital configuration relative to the Sun, known as the Milankovitch hypothesis, astronomical theory, or orbital forcing, have long been considered the leading theory for the primary mechanism driving Quaternary glacial-interglacial cycles (*1–3*) and associated climate change. The hypothesis is supported by a huge array of evidence from paleoclimate records across the globe, which show that major shifts in

Science

The 5300-year-old *Helicobacter pylori* genome of the Iceman

Frank Maixner, Ben Krause-Kyora, Dmitrij Turaev, Alexander Herbig, Michael R. Hoopmann, Janice L. Hallows, Ulrike Kusebauch, Eduard Egarter Vigl, Peter Malfertheiner, Francis Megraud, Niall O'Sullivan, Giovanna Cipollini, Valentina Coia, Marco Samadelli, Lars Engstrand, Bodo Linz, Robert L. Moritz, Rudolf Grimm, Johannes Krause, Almut Nebel, Yoshan Moodley, Thomas Rattei and Albert Zink

Stomach ache for a European mummy

Five thousand years ago in the European Alps, a man was shot by an arrow, then clubbed to death. His body was subsequently mummified by ice until glacier retreat exhumed him in 1991. Subsequently, this ancient corpse has provided a trove of intriguing information about copper-age Europeans. Now, Maixner *et al.* have identified the human pathogen *Helicobacter pylori* within the mummy's stomach contents. The strain the "Iceman" hosted appears to most closely resemble pathogenic Asian strains found today in Central and Southern Asia.
Science, this issue p. 162

ARTICLE TOOLS	http://science.sciencemag.org/content/351/6269/162
SUPPLEMENTARY MATERIALS	http://science.sciencemag.org/content/suppl/2016/01/06/351.6269.162.DC1
REFERENCES	This article cites 90 articles, 24 of which you can access for free http://science.sciencemag.org/content/351/6269/162#BIBL
PERMISSIONS	http://www.sciencemag.org/help/reprints-and-permissions

Use of this article is subject to the Terms of Service